X-ray Absorption Edge and EXAFS Studies of the Blue Copper Site in Stellacyanin: Effects of Axial Amide Coordination†

Serena DeBeer,‡ David W. Randall,‡ Aram M. Nersissian,§ Joan Selverstone Valentine,§ Britt Hedman,*,‡,|| Keith O. Hodgson,*,‡,|| and Edward I. Solomon*,‡

Contribution from Department of Chemistry, Stanford University, Stanford, California 94305, Department of Chemistry and Biochemistry, UCLA, Los Angeles, California 90095-1569, and Stanford Synchrotron Radiation Laboratory, SLAC, Stanford University, Stanford, California 94309

Received: April 6, 2000; In Final Form: June 1, 2000

The blue copper sites in *Cucumis sativus* stellacyanin and *Rhus vernicifera* stellacyanin have been investigated by X-ray absorption spectroscopy (XAS) in order to probe the effects of axial amide coordination. EXAFS results show a slight lengthening of the Cu−S(Cys) bond in both stellacyanins compared to the classic blue copper site in azurin. The 1s → 3d transition in the Cu K-edge of stellacyanin is ∼0.5 eV lower in energy than those of the classic blue copper sites, consistent with a stronger ligand donor set. A configuration interaction (CI) model applied to the 1s → 4p and 1s → 4p + shakedown transitions in the edge predicts less covalent bonding for stellacyanin than for plastocyanin, which is attributed to a weaker thiolate bond. These studies demonstrate that the strength of the axial ligand interaction inversely affects the strength of the thiolate−copper bond.

Introduction

Blue copper proteins exhibit high-redox potentials and rapid electron-transfer rates compared to "normal" tetragonal copper complexes.[1−5] They are characterized by unusual spectroscopic features, including an intense absorption band at ∼600 nm and a small $A_{||}$ value in the EPR spectra.[6,7] These features reflect novel electronic structures that play a key role in the long-range electron-transfer function of these proteins.[7−9]

Classic blue copper sites, such as azurin and plastocyanin, have a single Cu ion in a trigonally distorted tetrahedral environment.[3] The trigonal plane contains a single Cu ion with a very short Cu−S(Cys) and two typical Cu−N(His) distances. The axial ligand is usually a S(Met) having a long Cu−S bond length, which decreases its donor interaction with the Cu. This decrease is partially compensated for by a short, strong Cu−S(Cys) thiolate bond.[10] Direct evidence for the highly covalent Cu−S(Cys) interaction has been obtained through S K-edge studies on plastocyanin, which quantifies the S(Cys) π character in the Cu $d_{x^2-y^2}$ orbital as 38%.[11] This covalency can provide strong electronic coupling into protein pathways to facilitate rapid long-range electron transfer.[12]

Within the family of blue copper proteins, there are a number of proteins with "perturbed" sites, which exhibit spectral features that are substantially different from those of the classic blue copper sites in plastocyanin and azurin.[13,14] The perturbed blue copper sites can be divided into three different classes based on structural motifs and spectral properties. The first class includes sites in which the axial S(Met) is replaced by a stronger field ligand (e.g., O(Gln) in stellacyanin[15]) that distorts the Cu out of the trigonal plane producing a more tetrahedral geometry. The second class has the same ligand set as plastocyanin (e.g., nitrite reductase[16] and cucumber basic protein[17]); however, the changes in the UV-Vis absorption spectrum indicate that the Cu−S(Cys) interaction in the HOMO is rotating from a pure π to a more σ bonding interaction with the thiolate ligand and MCD spectra indicate a tetragonal distortion of the ligand field relative to that of plastocyanin.[13,14] The third class includes those blue sites in which the S(Met) is replaced with a Leu or Phe (as in the fungal laccases[18−20]), and hence no axial ligand is provided by the protein.[21]

This study focuses on the first class of perturbed blue copper sites, including *Cucumis sativus* stellacyanin and *Rhus vernicifera* stellacyanin. The 1.6-Å crystal structure of *C.s.* stellacyanin shows that the S(Met) of the classic blue copper sites is replaced by a short O(Gln) at ∼2.2 Å.[15] In addition, the Cu−S(Cys) bond is approximately ∼0.1 Å longer than that found in plastocyanin. On the basis of optical absorption, CD, MCD, and density functional calculations, it has been found that the larger axial interaction in stellacyanin weakens the thiolate interaction.[14] We are interested in further probing the effects of the axial amide coordination on the Cu−S(Cys) bond through Cu K-edge XAS studies. EXAFS studies provide a direct probe of changes in the Cu−S(Cys) bond length. Although previous XAS studies have been carried out on both classic blue copper proteins and on the perturbed site in stellacyanin, discrepancies exist in the literature as to whether the Cu−thiolate bond is approximately the same length as in plastocyanin[22] or if it is longer[23,24] (as indicated by crystallography). These discrepancies may result from the use of different fitting methods. It is therefore important to carry out EXAFS analyses using the same theoretical fitting protocol for both the classic and the perturbed sites, to obtain an accurate assessment of the changes that occur at the Cu site.

† Part of the special issue "Thomas Spiro Festschrift".

* To whom correspondence should be addressed: B. H. at Tel: 650-926-3052. Fax: 650-926-4100. Email: hedman@ssrl.slac.stanford.edu. K. O. H. at Tel: 650-926-3153; Fax: 650-926-4100; Email: hodgson@ssrl.slac.stanford.edu. E. I. S. at Tel: 650-723-9104; Fax: 650-725-0259; Email: edward.solomon@stanford.edu.

‡ Department of Chemistry, Stanford University, Stanford, California.

§ Department of Chemistry and Biochemistry, UCLA, Los Angeles, California.

|| Stanford Synchrotron Radiation Laboratory, SLAC, Stanford University, Stanford, California.

10.1021/jp001334d CCC: $19.00
Published on Web 08/23/2000

In addition, a systematic study at the Cu K-edge allows spectroscopic changes that result from the change in axial ligation to be clearly identified. Specifically, changes in the edge structure that reflect a stronger ligand donor set and a weaker thiolate−copper bond in stellacyanin will be discussed.

Experimental Section

Preparation of Protein Samples. *Rhus vernicifera* stellacyanin,[25] *Cucumis sativus* stellacyanin,[26] and *Pseudomonas aeruginosa* azurin[27] were prepared according to published procedures. The protein concentrations were 4.0 mM in 20 mM phosphate buffer, 6.0 mM in 5 mM acetate buffer, and 4.0 mM in 50 mM phosphate buffer for *R.v.* stellacyanin, *C.s.* stellacyanin, and *P.a.* azurin, respectively. All samples (ca. 120 μL) contained $\sim$ 50% glycerol as a glassing agent. The samples were loaded into 1-mm Lucite XAS cells with 63.5-μm Mylar windows and then frozen immediately by immersion in liquid nitrogen prior to the XAS measurements.

X-ray Absorption Measurements and Data Acquisition. All of the data were collected at the Stanford Synchrotron Radiation Laboratory (SSRL) on unfocused 8-pole wiggler beam line 7−3 under ring conditions 3.0 GeV and 60−100 mA. A Si(220) monochromator was utilized for energy selection at the Cu K-edge. The monochromator was detuned 50% to minimize higher harmonic components in the X-ray beam. The samples were maintained at 10 K during the data collection using an Oxford Instruments CF1208 continuous flow liquid helium cryostat. Data were measured in fluorescence mode using either a Canberra Ge 13-element array detector (for concentrations < 5 mM) or an Ar-filled ionization chamber[28,29] detector equipped with a Ni filter and Soller slits (for concentrations > 5 mM). XAS data were measured to $k = 13.4$ Å^{-1} (the zinc K-edge), as all samples were found to contain a small amount of zinc. The internal energy calibration was performed by simultaneous measurement of the absorption of a Cu foil placed between a second and third ionization chamber. The first inflection point of the Cu foil was assigned to 8980.3 eV. All of the samples were monitored for photoreduction throughout the course of data collection. Only those scans that showed no evidence of photoreduction were used for edge comparisons. For the EXAFS analysis, only scans that showed less than 5% photoreduction (10 scans for *R.v.* stellacyanin, 14 scans for *C.s.* stellacyanin, and 10 scans for *P.a.* azurin) were averaged.

XAS Data Analysis. The averaged data were processed as described previously[30] by fitting a second-order polynomial to the post-edge region and subtracting this background from the entire spectrum. A three-region cubic spline was used to model the smooth background above the edge. Normalization of the data was achieved by subtracting the spline and normalizing the edge jump to 1.0 at 9000 eV. The resultant EXAFS was k^3-weighted to enhance the impact of high-k data.

Theoretical EXAFS signals $\chi(k)$ were calculated using FEFF (version 6.0)[31,32] and fit to the data using EXAFSPAK (G. N. George, SSRL). The experimental energy threshold, E_o (the point at which, $k = 0$), was chosen as 8990 eV. The structural parameters that were varied during the refinements include the bond distance (R) and the bond variance (σ^2). The σ^2 is related to the Debye−Waller factor, which is a measure of thermal vibration and static disorder of the absorbers/scatterers. Coordination numbers were systematically varied in the course of the analysis, but they were not allowed to vary within a given fit. Single scattering paths and the corresponding multiple scattering paths were linked during the course of refinements.

Fits to the edges were performed using the program EDG_FIT (G. N. George, SSRL). The data were fit using three psuedo-Voigt peaks and an arc-tangent to simulate the edge jump. Second derivative spectra were used as guides to determine the number and position of peaks. For all fits, the energies, amplitudes, and half-widths were allowed to vary. Fits were performed in which the position of the arc-tangent was systematically varied (the arc-tangent could vary $\sim$0.7 eV and still give a reasonable fit); these fits indicate that the position of the arc-tangent can introduce $\sim$10% error in the I_M/I_S ratio.

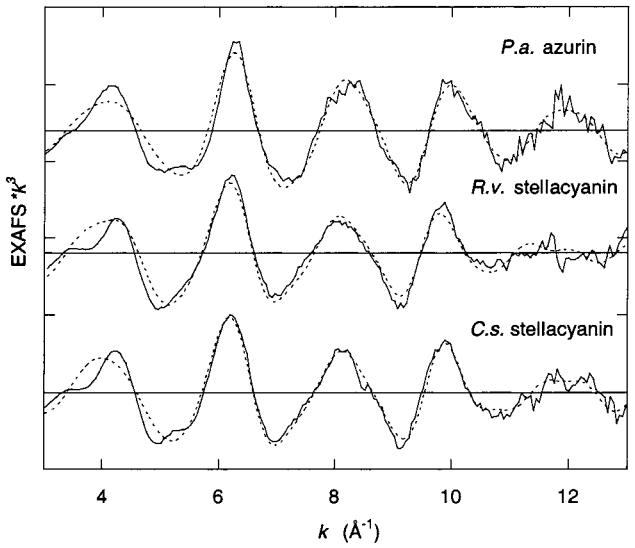

Figure 1. Experimental EXAFS data (—) and fits to the data (- - -) for *P.a.* azurin, *R.v.* stellacyanin, and *C.s.* stellacyanin. (Each major tick on the ordinate scale represents 5 units.)

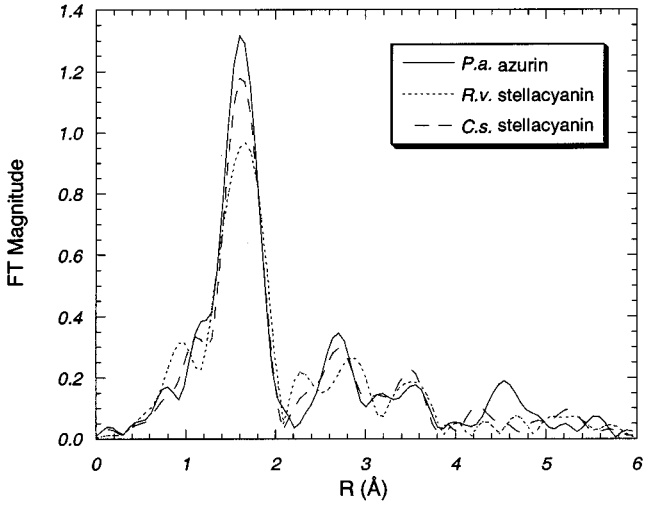

Figure 2. Non-phase shift corrected Fourier transforms for *P.a.* azurin, *R.v.* stellacyanin, and *C.s.* stellacyanin.

Results and Analysis

EXAFS. The k^3-weighted EXAFS data and fits for *P.a.* azurin and *R.v.* and *C.s.* stellacyanin are shown in Figure 1. A comparison of the corresponding FTs is shown in Figure 2. The EXAFS signals of *C.s* and *R.v.* stellacyanin are, as expected, very similar. There are changes in the first shell FT amplitude of the two forms of stellacyanin that most likely results from a slightly different distribution of the first shell Debye−Waller values (Table 1). The EXAFS data for azurin show subtle differences relative to the two stellacyanin samples. These differences, as they relate to the fit results, will be considered below.

TABLE 1: A Comparison of EXAFS Fit Results

	R.v. Stellacyanin		*C.s.* Stellacyanin		*P.a.* Azurin	
	R(Å)	σ^2 (Å^2)	R (Å)	σ^2 (Å^2)	R (Å)	σ^2 (Å^2)
2 Cu−N	1.95	0.0041	1.96	0.0025	1.95	0.0021
1 Cu−S	2.18	0.0028	2.17	0.0041	2.14	0.0036
4 Cu−C2/C5[a]	2.97	0.0051	2.96	0.0042	2.92	0.0051
4 Cu−N−C2/C5	3.17	0.0051	3.18	0.0042	3.18	0.0051
4 Cu−C3/N4[a]	4.00	0.0105	3.92	0.0041	3.89	0.0081
4 Cu−N−C3/N4	4.23	0.0091	4.23	0.0041	4.11	0.0083
Normalized error[b]		0.304		0.277		0.324

[a] These components represent a single scattering path (top) and the corresponding multiple scattering path (bottom). [b] Error is given by $\sum[(\chi_{obsd} - \chi_{calcd})^2 k^6]/\sum[(\chi_{obsd2} k^6]$.

FEFF fits to oxidized *R.v.* and *C.s.* stellacyanin were performed using the 1.6-Å crystal structure of oxidized *C.s.* stellacyanin as a starting model. A good fit to *R.v.* stellacyanin was obtained by including 1 Cu−S at 2.18 Å and 2 Cu−N interactions at 1.95 Å. Multiple scattering interactions from the imidazole rings of the ligating histidines were necessary to fit the outer shells. Very similar fit results were obtained for *C.s.* stellacyanin (Table 1). In both cases, a short Cu−O, corresponding to the axial glutamine seen in the crystal structure, could be included at 2.20 Å. This resulted in a decrease in the Cu−N and Cu−S Debye−Waller values and only a slight decrease in the fit error. Hence, on the basis of the EXAFS results alone, there is no definitive evidence for the presence of the short axial Cu−O interaction. However, Cu−K edge studies (vide infra) indicate a stronger ligand donor set in stellacyanin as compared to plastocyanin and azurin, which is likely due to the stronger axial interaction of the O(Gln) as compared to S(Met).

FEFF fits to oxidized azurin were performed using the 1.9-Å crystal structure of oxidized *P.a.* azurin as a starting model.[33] A good fit to oxidized azurin was obtained by including 1 Cu−S at 2.14 Å and 2 Cu−N interactions at 1.95 Å (Table 1). The outer shells were well fit by including Cu−N−C/N multiple scattering interactions from the two ligating imidazoles. Fit results showed no evidence for the distant axial 3.1 Å S(Met) or 3.0 Å O(Gly),[33] which is to be expected as such weakly interacting atoms would not necessarily contribute significantly to the EXAFS signal.

A comparison of the EXAFS fit results for stellacyanin and azurin shows that the changes at the copper site are very subtle. The Cu−N(His) distances do not change. The Cu−S(Cys) bond is increased by 0.03−0.04 Å in stellacyanin. Within the error limits of EXAFS, this change is small; however, the trend is consistent for both stellacyanins and parallels that observed in resonance Raman spectroscopy. The intensity-weighted average frequency for the Cu−S stretch is 409, 378, and 386 cm^{-1}, for plastocyanin, *R.v.* and *C.s.* stellacyanin, respectively.[34] Applying Badger's rule[35] and using the 2.07 Å Cu−S distance from the 1.3-Å crystal structure of plastocyanin as a reference,[36] predicts Cu−S distances of 2.18 and 2.15 Å, for *R.v.* and *C.s.* stellacyanin, respectively.

Cu K-Edges. A comparison of the Cu K-edge spectra of spinach plastocyanin,[11] *P.a* azurin, and *C.s.* stellacyanin is shown in Figure 3a, and the corresponding second derivatives in Figure 3b. The edges of *C.s.* and *R.v.* stellacyanin are essentially identical (Supporting Information, Figure S1), and therefore, for clarity, the edge of *R.v.* stellacyanin is not shown. In all 3 proteins, there are at least 4 transitions that are superimposed on the rising edge, one at ∼8979 eV, two in the region between 8984 and 8987 eV, and one at ∼8992 eV.

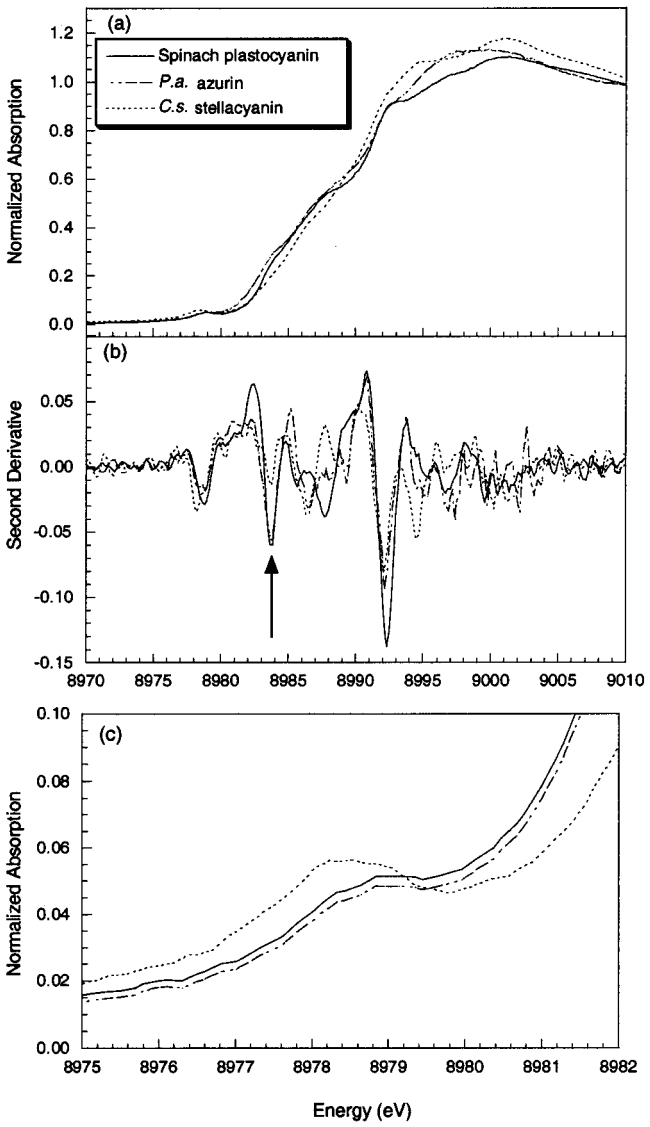

Figure 3. (a) Comparison of the normalized Cu K-edge XAS spectra of spinach plastocyanin (—), adapted from ref 11, azurin (— - - —) and stellacyanin (- - -). (b) Second derivative of the data shown in (a). The arrow marks the 1s → 4p + shakedown feature. (c) Expanded pre-edge region of the data shown (a).

Analysis of 1s → 3d Pre-edge Transitions. The peak at ∼8979 eV corresponds to a Cu 1s → 3d pre-edge transition. As shown in Figure 3c, the energy of the pre-edge in stellacyanin is shifted down by ∼0.5 eV relative to that of the classic blue copper sites. There are two main factors that can contribute to the shift in the pre-edge. The first is a change in the ligand field. On the basis of MCD studies, the ligand field of stellacyanin is decreased relative to plastocyanin.[14] This results in a decrease in the d → d energies of ∼1600 cm^{-1} (or ∼ 0.2 eV) and can thus account for part of the energy shift seen in the pre-edge. The remaining shift of ∼0.3 eV may be attributed to the decreased Z_{eff} in stellacyanin due to a stronger ligand donor set associated with the short axial amide replacing the long S(Met) thioether. A decrease in Z_{eff} would have a greater effect on the energy of the 1s core orbital than on the d-manifold.[37] Thus, the splitting between the 1s and 3d orbitals decreases with a decrease in Z_{eff}. This is further supported by the shifts in the transition at ∼8992 eV. This transition, which likely corresponds to the main 1s → 4p transition (vide infra), is shifted to lower energy (by ∼0.2 eV) in stellacyanin and thus supports the 1s core of stellacyanin being to lower binding energy.

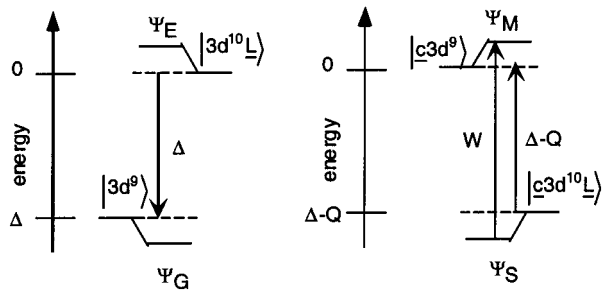

Figure 4. Configuration interaction model for analysis of Cu K-edge data: (left) ground-state configurations and (right) relaxed final state configurations.

Analysis of 1s → 4p Edge Transitions. The transition at ~8984 eV has been previously assigned as a 1s → 4p transition with concurrent ligand-to-metal charge transfer,[38,39] which gains intensity through final state relaxation (i.e., formally a 2-electron shakedown transition). As can be most clearly seen from the second derivative in Figure 3b (arrow), on going from plastocyanin or azurin to stellacyanin, the intensity of the shakedown feature is decreased relative to the intensity of the main peak at ~8992 eV. To interpret the change in relative intensities, a valence bond configuration interaction (VBCI) model was applied to the data, as described by Sawatzky, et al.[40] and Davis.[41] This model has previously been applied to both PES[42] and XAS[11] data in order to quantify covalency. In a K-edge absorption process, a 1s core hole is formed in the ground configuration (Ψ_G). In the sudden approximation, the creation of the core hole occurs rapidly, before the remaining electrons adjust to the new potential. The intensity I_i of a given transition i, corresponding to either the main or shakedown final state, can then be expressed as

$$I_i = |\langle \Psi^{n-1}{}_i\,(\underline{c})|\Psi^{n-1}{}_R\,(\underline{c})\rangle|^2 \tag{1}$$

where $\underline{c}$ denotes a core hole, Ψ_i denotes the relaxed final states (main or shakedown), and Ψ_R is the initial unrelaxed state with the core electron removed. This requires that only initial and final states with the same symmetry can contribute to shakedown intensity.

In the VBCI model, the ground-state wave function Ψ_G is obtained from diagonalization of the matrix:

	$\lvert 3d^9\rangle$	$\lvert 3d^{10}\underline{L}\rangle$
$\langle 3d^9\rvert$	Δ	T
$\langle 3d^{10}\underline{L}\rvert$	T	0

(2)

$|3d^9\rangle$ is the metal electron valence configuration, $|3d^{10}\underline{L}\rangle$ represents the one-electron ligand-to-metal charge-transfer configuration before mixing, and $\underline{L}$ denotes a ligand hole. Δ is the energy difference between the two configurations before CI, Figure 4. T is the interaction matrix element between the configurations contributing to the ground-state wave function. Diagonalization gives the eigenvector corresponding to the lowest energy state as

$$\Psi_G = \cos\theta|3d^9\rangle - \sin\theta|3d^{10}\underline{L}\rangle \tag{3}$$

where

$$\tan 2\theta = 2T/\Delta \tag{4}$$

Δ is by this definition negative.

The 1s → 4p transition and the corresponding creation of the core hole produces two possible final states corresponding to a main (Ψ_M) and a shakedown (Ψ_S) peak at lower energy. The energy matrix for the excited states is constructed in a manner analogous to the ground state, with the addition of a term Q to the diagonal energy of the $\underline{c}3d^9$ configuration to account for the increase in effective nuclear charge felt by the $3d^9$ state due to the creation of a core hole. The solution for the excited-state wave functions are given by

$$\Psi_M = \sin\theta'|\underline{c}3d^9\rangle + \cos\theta'|\underline{c}3d^{10}\underline{L}\rangle \tag{5a}$$

$$\Psi_S = \cos\theta'|\underline{c}3d^9\rangle - \sin\theta'|\underline{c}3d^{10}\underline{L}\rangle \tag{5b}$$

where

$$\tan 2\theta' = 2T/(\Delta - Q) \tag{6}$$

The energy splitting W between the main peak and the shakedown peak is given by

$$W = [(\Delta - Q)^2 + 4T^2]^{1/2} \tag{7}$$

The intensity ratio for the main-to-shakedown peak is given by

$$\frac{I_M}{I_S} = \frac{\sin\theta'\cos\theta - \cos\theta'\sin\theta}{\cos\theta'\cos\theta + \sin\theta'\sin\theta} = \tan^2(\theta' - \theta) \tag{8}$$

Equations 4, 6, 7, and 8 form a system of 4 equations and 7 unknowns. Three of these (Δ, T, and θ) refer to the ground-state metal−ligand interaction, two to the excited state (Q and θ') and two to experimental observables (W and I_M/I_S). Typically, W and I_M/I_S are measured directly from spectra and a third variable is obtained from a complementary method. This allows for the system of four equations to be solved to determine the remaining variables.

An approach similar to that used in ref 11 in the analysis of the Cu K-edge data of D_{4h} $CuCl_4^{2-}$ was used in this study. Because z-polarized Cu K-edge data are available for plastocyanin (Figure 5A),[11] these were first used to test the transferability of this method to non-polarized edges. The z-polarized data reflect the 1s → $4p_z$ transition probability, which should occur at lower energy than the 1s → $4p_{x,y}$ transition in a planar system due to the lack of ligand field repulsion along the z axis. Thus, the z-polarized peak positions and intensities are the major contribution to the low-energy region of the orientation averaged edges. However, it was found that the difficulty in simulating the background rising edge absorption as well as a contribution from an additional shakedown in the region between 8985 and 8990 eV in Figure 5a led to imprecision in the determination of I_M/I_S. For this reason, I_M/I_S was treated as an unknown. Ground-state parameters Δ and T were chosen such that the energy splitting in the initial state and the coefficients of the ground-state wave functions were consistent with the optical absorption data and the results of DFT calculations.[13,43] This corresponds to $\Delta = -0.4$ eV and $T = -1.0$ eV. These values, together with the measured separation between the two peaks (W), were used to calculate the remaining four parameters. Solving the set of four equations, using $\Delta = -0.4$ eV, $T = -1.0$ eV, and $W = 8.1$ eV, resulted in a set of predicted values for θ, θ', Q, and I_M/I_S (Table 2). These results are compared to the Cu K-edge data in Table 3 (top row) and Figure 5a. The calculated intensity ratio for plastocyanin ($I_M/I_S = 0.90$) is in

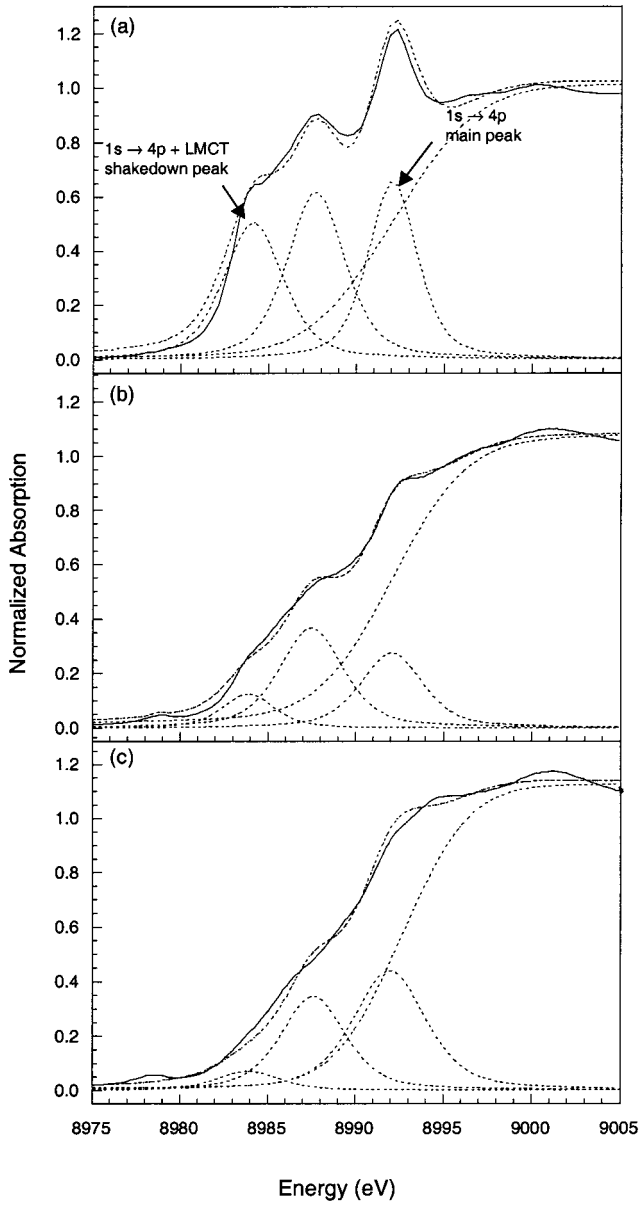

Figure 5. Fits to the Cu K-edges of (a) *z*-polarized plastocyanin, (b) orientation averaged plastocyanin, and (c) stellacyanin.

reasonable agreement with the value estimated for the *z*-polarized plastocyanin data ($I_M/I_S = 1.1$, Table 3, Figure 5a). However, the fits to the isotropic data in Figure 5b show that the intensity of the shakedown feature is greatly reduced relative to the main peak. This is due to a significant contribution from the *x,y*-polarized 1s → $4p_{x,y}$ main and shakedown transitions, which contribute in the 8995−9000 eV region in Figure 5b, increasing the relative intensity of the main peak. If, the *x,y* contribution is taken to be approximately equal in plastocyanin and stellacyanin, the relative I_M/I_S ratios can still be compared. As shown in Table 3, Figures 5c and S2, the I_M/I_S ratio is much larger for both forms of stellacyanin than for plastocyanin, whereas the splitting between the main and shakedown peaks (W) in unchanged.[44] The CI-model calculations show that decreasing the value of T best accounts for this change. This results in an increase in the d-character of the ground state in stellacyanin indicating a less covalent bonding interaction. This is consistent with the results of Xα-calculations[14] and resonance Raman data, which predict a weaker Cu−S(Cys) bond.

TABLE 2: Results of CI Model Calculation for Plastocyanin and Stellacyanin

	Plastocyanin	Stellacyanin
Δ	−0.4	−0.4
T	−1.0	−0.6
Q	−8.29	−8.37
$\cos^2\theta * 100$	59.8%	65.8%
$\cos^2\theta' * 100$	1.5%	0.6%
W	8.14	8.06
I_M/I_S	0.90	1.41

TABLE 3: Representative Fit Results for the Cu K-Edge Spectra of *z*-polarized Plastocyanin and of Non-polarized Plastocyanin, *P.a.* Azurin, *C.s.* Stellacyanin, and *R.v.* Stellacyanin

	peak 1 (shakedown)	peak 2	peak 3 (main peak)	arctan/ erf	W (eV)	I_M/I_S
			z-polarized plastocyanin			
energy (eV)	8984.1	8987.7	8992.1	8992.1	8.0	1.07
amplitude	0.51	0.62	0.66	1.00		
hwhm	2.01	1.94	1.64	6.12		
			non-polarized plastocyanin			
energy (eV)	8983.9	8987.5	8992.1	8992.1	8.1	2.78
amplitude	0.12	0.38	0.28	1.05		
hwhm	1.76	2.15	2.10	5.04		
			non-polarized *P.a.* azurin			
energy (eV)	8983.9	8987.5	8992.1	8992.1	8.1	2.59
amplitude	0.16	0.33	0.26	1.06		
hwhm	1.96	2.39	3.12	5.00		
			non-polarized *C.s.* stellacyanin			
energy (eV)	8983.9	8987.6	8991.9	8992.7	8.1	6.00
amplitude	0.08	0.35	0.44	1.07		
hwhm	2.23	2.20	2.43	4.94		
			non-polarized *R.v.* stellacyanin			
energy (eV)	8983.9	8987.6	8991.9	8992.7	8.1	6.32
amplitude	0.08	0.35	0.44	1.07		
hwhm	2.13	2.19	2.45	4.84		

Discussion

The XAS data for stellacyanins are in agreement with the oxidized crystal structure of *C.s.* stellacyanin.[15] The EXAFS data are well fit by the inclusion of 1 Cu−S(Cys) at ∼2.2 Å and 2 Cu−N(His) at ∼2.0 Å, with presence of two histidine ligands further evidenced by the improved fit to the data upon inclusion of multiple scattering contributions from two imidazole rings. The EXAFS analyses provide no direct evidence for the short Cu−O(Gln) seen in the crystal structure. However, the decrease in the 1s → 3d pre-edge transition energy by ∼0.5 eV relative to azurin and plastocyanin provides evidence for an additional strong donor. For both stellacyanins, the EXAFS data show a slight increase in the Cu−S(Cys) bond (0.03−0.04 Å) as compared to the classic blue copper site in azurin. The increased Cu−S(Cys) bond length is attributed to the increased donor interaction of the axial O(Gln) in stellacyanin as compared to the relatively weak S(Met) donor in azurin.

Further evidence for a weakened Cu−S(Cys) thiolate bond is provided by the Cu K-edges. The results of a CI analysis applied to the 1s → 4p and 1s → 4p + shakedown transitions in the edge predicts less covalent bonding for stellacyanin than for plastocyanin. Hence, our studies clearly demonstrate that the strength of the axial ligand interaction inversely affects the strength of the thiolate−copper bond.

Acknowledgment. This work was supported by NIH RR-01209 (K.O.H), NIH GM28222 (J.S.V.), and NSF CHE-9528250 (E.I.S.). SSRL operations are funded by the Department of Energy, Office of Basic Energy Sciences. The Structural Molecular Biology program is supported by the National

Institutes of Health, National Center for Research Resources, Biomedical Technology Program and by the Department of Energy, Office of Biological and Environmental Research.

Supporting Information Available: Comparison of the normalized Cu K-edge XAS spectra of *R.v.* stellacyanin and *C.s.* stellacyanin. Fits to the Cu K-edges of *R.v.* stellacyanin and *P.a.* azurin. This material is available free of charge via the Internet at http://pubs.acs.org.

References and Notes

(1) Gray, H. B.; Solomon, E. I. In *Copper Proteins*; Spiro, T. G., Ed.; Wiley: New York, 1981; pp 1−39.

(2) Adman, E. T. In *Topics in Molecular and Structural Biology*: *Metalloproteins*; Harrison, P., Ed.; Macmillan: New York, 1985; Vol. 1, pp 1−42.

(3) Adman, E. T. *Adv. in Prot. Chem.* **1991**, *42*, 145−197.

(4) Sykes, A. G. *Adv. Inorg. Chem.* **1991**, *107*, 377−408.

(5) Messerschmidt, A. *Struct. Bonding* **1998**, *90*, 37−68.

(6) Penfield, K. W.; Gewirth, A. A.; Solomon, E. I. *J. Am. Chem. Soc.* **1985**, *107*, 4519−4529.

(7) Solomon, E. I.; Baldwin, M. J.; Lowery, M. D. *Chem. Rev.* **1992**, *92*, 521−542.

(8) Randall, D. W.; Gamelin, D. R.; LaCroix, L. B.; Solomon, E. I. *J. Biol. Inorg. Chem.* **2000**, *5*, 16−29.

(9) Solomon, E. I.; Randall, D. W.; Glaser, T. *Coord. Chem. Rev.*, in press.

(10) Guckert, J. A.; Lowery, M. D.; Solomon, E. I. *J. Am. Chem. Soc.* **1995**, *117*, 2817−2844.

(11) Shadle, S. E.; Penner-Hahn, J. E.; Schugar, H. J.; Hedman, B.; Hodgson, K. O.; Solomon, E. I. *J. Am. Chem. Soc.* **1993**, *115*, 767−776.

(12) Lowery, M. D.; Guckert, J. A.; Gebhard, M. S.; Solomon, E. I. *J. Am. Chem. Soc.* **1993**, *115*, 3012−3013.

(13) LaCroix, L. B.; Shadle, S. E.; Wang, Y. N.; Averill, B. A.; Hedman, B.; Hodgson, K. O.; Solomon, E. I. *J. Am. Chem. Soc.* **1996**, *118*, 7755−7768.

(14) LaCroix, L. B.; Randall, D. W.; Nersissian, A. M.; Hoitink, C. W. G.; Canters, G. W.; Valentine, J. S.; Solomon, E. I. *J. Am. Chem. Soc.* **1998**, *120*, 9621−9631.

(15) Hart, P. J.; Nersissian, A. M.; Herrmann, R. G.; Nalbandyan, R. M.; Valentine, J. S.; Eisenberg, D. *Prot. Sci.* **1996**, *5*, 2175−2183.

(16) Adman, E. T.; Godden, J. W.; Turley, S. *J. Biol. Chem.* **1995**, *270*, 27 458−27 474.

(17) Guss, J. M.; Merritt, E. A.; Phizackerley, R. P.; Freeman, H. C. *J. Mol. Biol.* **1996**, *259*, 686−705.

(18) Xu, F.; Shin, W.; Brown, S. H.; Wahleithner, J.; Sundaram, U. M.; Solomon, E. I. *Biochim. Biophys. Acta* **1996**, *1292*, 303−311.

(19) Messerschmidt, A.; In Multicopper Oxidases Messerschmidt, A., Ed.; World Scientific: Singapore, 1997; pp 23−80.

(20) Germann, U. A.; Müller, G.; Hunziker, P. E.; Lerch, K. *J. Biol. Chem.* **1988**, *263*, 885−896.

(21) Ducros, V.; Brzozowski, A. M.; Wilson, K. S.; Brown, S. H.; Ostergaard, P.; Schneider, P.; Yaver, D. S.; Pedersen, A. H.; Davies, G. J. *Nat. Struct. Biol.* **1998**, *5*, 310−316.

(22) Strange, R. W.; Reinhammar, B.; Murphy, L. M.; Hasnain, S. S. *Biochemistry* **1995**, *34*, 220−231.

(23) Feiters, M. C.; Dahlin, S.; Reinhammer, B. *Biochim. Biophys. Acta* **1988**, *955*, 250−260.

(24) Peisach, J.; Powers, L.; Blumberg, W. E.; Chance, B. *Biophys. J.* **1982**, *38*, 277−285.

(25) Reinhammar, B. *Biochim. Biophy. Acta* **1970**, *205*, 34−47.

(26) Nersissian, A. M.; Mehrabian, Z. B.; Nalbandyan, R. M.; Hart, P. J.; Fraczkiewicz, G.; Czernuszewicz, R. S.; Bender, C. J.; Peisach, J.; Herrmann, R. G.; Valentine, J. S. *Protein Science* **1996**, *5*, 2184−2192.

(27) Karlsson, B. G.; Pascher, T.; Nordling, M.; Arvidsson, R. H. A.; Lundberg, L. G. *FEBS Lett.* **1989**, *246*, 211−217.

(28) Stern, E. A.; Heald, S. M. *Rev. Sci. Instrum.* **1979**, *50*, 1579−1582.

(29) Lytle, F. W.; Greegor, R. B.; Sandstrom, D. R.; Marques, E. C.; Wong, J.; Spiro, C. L.; Huffman, G. P.; Huggins, F. E. *Nucl. Instrum. Methods* **1984**, *226*, 542−548.

(30) DeWitt, J. G.; Bentsen, J. G.; Rosenzweig, A. C.; Hedman, B.; Green, J.; Pilkington, S.; Papaefthymiou, G. C.; Dalton, H.; Hodgson, K. O.; Lippard, S. J. *J. Am. Chem. Soc.* **1991**, *113*, 9219−9235.

(31) Rehr, J. J.; Mustre de Leon, J.; Zabinsky, S. I.; Albers, R. C. *J. Am. Chem. Soc.* **1991**, *113*, 5135−5140.

(32) Mustre de Leon, J.; Rehr, J. J.; Zabinsky, S. I.; Albers, R. C. *Phys. Rev. B* **1991**, *44*, 4146−4156.

(33) Nar, H.; Messerschmidt, A.; Canters, G. W. *J. Mol. Biol.* **1991**, *221*, 765−772.

(34) Randall, D. W.; Solomon, E. I., unpublished results.

(35) Hershbach, D. E.; Laurie, V. W. *J. Chem. Phys.* **1961**, *35*, 458−463.

(36) Guss, J. M.; Bartunik, H. D.; Freeman, H. C. *Acta Crystallogr.* **1992**, *B48*, 790−811.

(37) For similar ligand sets, an increase in oxidation state of one unit is generally found to shift pre-edges up in energy by 1.0−1.5 eV. (Westre, T. E.; Kennepohl, P.; DeWitt, J. G.; Hedman, B.; Hodgson, K. O.; Solomon, E. I. *J. Am. Chem. Soc.* **1997**, *119*, 6297. DuBois, J. L.; Mukherjee, P.; Collier, A. M.; Mayer, J. M.; Solomon, E. I.; Hedman, B.; Stack, T. D. P.; Hodgson, K. O. *J. Am. Chem. Soc.* **1997**, *119*, 8578. Brant, P.; Stephens, P. A.; Solomon, E. I., to be published.) This reflects a larger shift in the core orbital binding energies relative to the valence with the removal of valence electron density and is attributed to electron repulsion.

(38) Bair, R. A.; Goddard, W. A., III *Phys. Rev. B* **1980**, *22*, 2767−2776.

(39) Kosugi, N.; Yokoyama, T.; Asakura, K.; Kuroda, H. *Chem. Phys.* **1984**, *91*, 249−256.

(40) van der Laan, G.; Westra, C.; Haas, C.; Sawatzky, G. A. *Phys. Rev. B.* **1981**, *23*, 4369−4380.

(41) Davis, L. C. *Phys. Rev. B.* **1982**, *25*, 2912−2915.

(42) Gewirth, A. A.; Cohen, S. L.; Schugar, H. J.; Solomon, E. I. *Inorg. Chem.* **1987**, *26*, 1133−1146.

(43) Gewirth, A. A.; Solomon, E. I. *J. Am. Chem. Soc.* **1988**, *110*, 3811−3819.

(44) Fit parameters were also determined for *P.a.* azurin (Table 3, Figure S3) and indicate that the I_M/I_S ratio is very similar to that in plastocyanin.